Chapter 1

Introduction

This report documents the design, testing and building of a stereoscopic mapping robot. The end product will be a small, two wheeled robot with a roller ball, that will autonomously search and map an unknown area and produce an occupancy map of the searched area.

An occupancy map is a representation of an area where a location is given a value of either *free, occupied* or *unkown* (Thrun (2003)). Three dimensional occupancy maps can also be generated, such as the OctoMap (Wurm et al. (2010)). Objects can also be tracked using an occupancy map and statistics (Fleuret et al. (2007)).

The purpose of a mapping robot is to build a representation of the area around it. This then facilitates the use of any application that requires prior knowledge of the area. One algorithm that is used to build up an occupancy map is the S.L.A.M. algorithm (Thrun and Montemerlo (2006)) and is used in other mapping robots(Se et al. (2002)). Accurate mapping robots tend to use laser range finders (Ruhnke et al. (2011)).

Stereoscopy in computer vision is the ability to calculate the locations and depths using images from two or more cameras, which are used to triangulate and estimate distances (Saxena et al. (2007)). By using two cameras on the same plane, separated by a set horizontal distance, the depth of the observed scene can be perceived by the system.

Stereovision is a small section of computer vision which is widely used in many applications, including Microsoft's Xbox Kinect (Microsoft (2012)), where stereo vision is used to locate a game player in order to use their movements to control

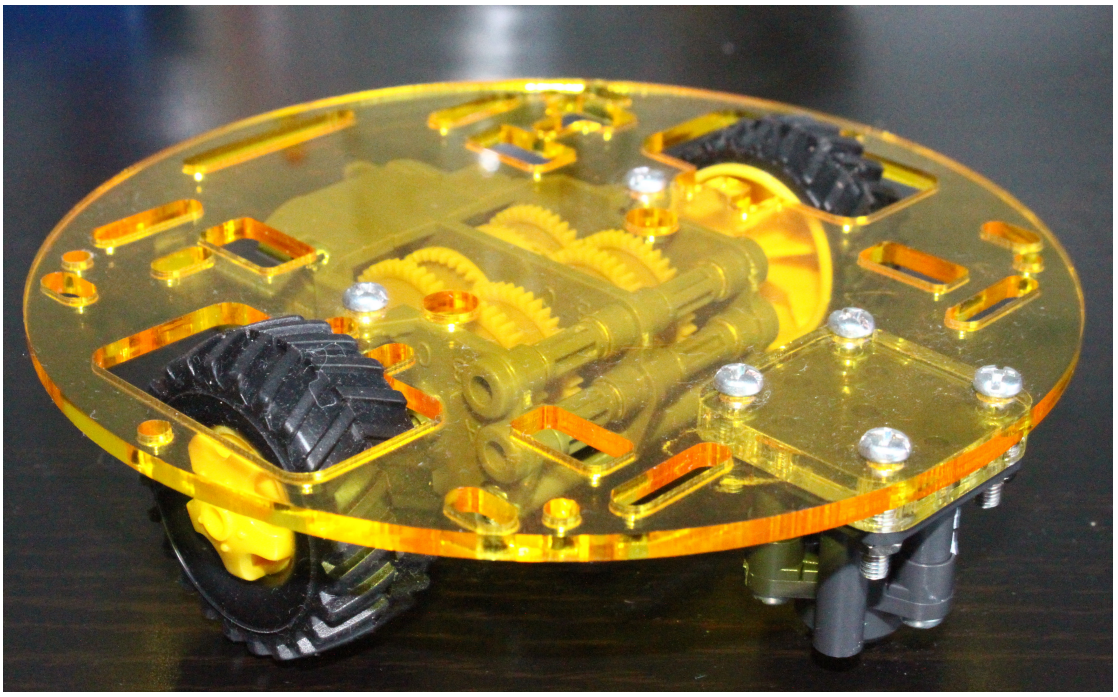

Figure 1.1: The base of the robot

the game. Mrovlje and Vrančić (2008) uses stereovision to be able to locate the distance to a marker.

The stereovision mapping robot discussed in this report is a low cost alternative to other robots which use laser range finders or high quality cameras (Se et al. (2002)). The robot will use the base seen in figure 1.1 and use two OmniVision OV7670 cameras delivering QVGA format images.

1.1 Project Management

In order to reduce the risk within the project, all aspects of potential issues are looked at and are summarised in table 1.1. A Gantt chart of how time will be spent can be seen in figure A.1.

The project will be designed in stages - first, gaining operation of all the basic sections; movement, image capturing, image detection algorithms etc. These will then be brought together once tested to create the final product.

Risk	Severity	Prevention
Parts not arriving on time	High	Order parts as early as possible
Project not fulfilling specification	High	Develop in stages to obtain functionality in parts. Ensure enough time is allocated to the project.
PCB Design is incorrect	Medium	Check the design carefully and get second opinion
Failure of personal computer causing data loss	Low	Keep back ups of all work on Devtrack Git repository and Dropbox.

Table 1.1: A list of risks and the prevention steps taken to reduce their impact

Chapter 2

Research

The research for this project was split into three sections:

1. Hardware
2. Software, broken down into:
   (a) Firmware, and
   (b) Algorithms

Hardware and firmware research will be discussed in this section. Vision algorithms are looked at in detail in chapter 4.

2.1 Hardware Research

2.1.1 Microcontrollers

The robot is to be designed with a budget of £80 (not including P.C.B.). The choice of microcontroller will be an important one, as a compromise between cost, power and usability must be made. There are two main brands of microcontrollers present in the consumer market: ARM and Atmel AVRs.
ARM is an architecture which is developed by ARM Holdings. ARM devices come in a many varieties: ARM9, ARM7, Strong ARM, ARM Cortex etc. Whilst ARM Holdings do not fabricate and sell the devices themselves, many companies, such as Texas Instruments, use the architecture and manufacture their own devices.

ARM cores are based on a RISC Harvard architecture and tend to be 32-bit with a high clock speed. ARM microcontrollers have onboard support for SPI, I^2C , PWM, ADCs and can have Flash, SRAM and EEPROM memory built-in. For this comparison, the Stellaris by Texas Instruments will be examined.

Atmel have a variety of products in the microcontroller market. They range from 8-bit, low clock speed devices for the hobbyist (ATMega and ATTiny series), to an improved 8-bit variant (XMega), and a 32-bit design (AT32UC3). XMegas and AVR32s tend to have higher clock speeds than the ATMegas. The AVR core also has a Harvard RISC architecture, and is mainly 8-bit. Atmel devices often have on board peripherals such as I^2C (called TWI on AVRs), SPI and ADCs, as well as a number of different memories: Flash, EEPROM and SRAM. An AT32UC3C0512C, ATXmega256A3BU and ATMega644P will be compared in this section.

Table 2.1 shows a brief summary of some common ARM and AVR microcontrollers. The Stellaris offers the most power with the largest DMIPS performance. However, due to the necessity of floating point operations, the AT32 clearly has a distinct advantage by having a built-in floating point unit. The XMega and ATMega do not offer enough power and are restricted by a small amount of SRAM and Flash. All devices looked at use 3.3V supply and have basic communication protocols (SPI, I^2C and USART). Overall, the AT32UC3C0512C is the best choice with a high throughput, a floating point unit and a vast amount of GPIO and communications. There is no EEPROM which may be desirable, but these can be added onto an SPI or I^2C bus. This device, although slightly more costly, is best suited to this application out of the selection researched.

2.2 Firmware

2.2.1 Camera

The camera used is the OV7670 camera by OmniVision. Steve Gunn provided source code for use on the Il Matto development board which uses an ATMega644P and also has an onboard SD Card reader. The original code streamed video from the camera to a colour TFT screen. The camera is supplied on a small breakout board with a FIFO buffer. The camera operation is discussed in section 3.1. Many implementations of firmware for this camera exist.

	ARM Stellaris	AT32UC3C0512C	XMegaA3BU	ATMega644P
Clock Speed (MHz)	80	33 or 66	32	12
DMIPS	100	91	-	20 MIPS
Package	100 LQFP or 108 BGA	64, 100, 144TQFP	64 QFP or QFN	40 DIP, 44 TQFP, 44 QFN
Cost of 1 unit(£)	10.30	15.39	6.65	6.86
Flash Size(kB)	256	512	256	64
SRAM Size (kB)	32	64	16	4
EEPROM Size(kB)	2	None internal	4	2
GPIO	64	45, 81 or 123	47	32
Operating Voltage (V)	3.3	5 or 3.3	1.6- 3.6[1]	2.7-5.5
Communication Interfaces	SPI, I^2C , SSI, MAC, CAN, EPI, USB, USART, I2S	SPI, TWI, EBI, USB, Ethernet, CAN, USART, I2S	USART, TWI, USB, SPI	SPI, TWI, USART
Floating Point	None	Built in FPU	None	None
ADCs	16	16	16	8
Timers	4	3 16-bit	7 16-bit, 8 8-bit	2 8-bit, 1 16-bit

Table 2.1: Comparison Table of some common microcontrollers. Data of microcontrollers taken from Atmel Corporation (2012a), Atmel Corporation (2012b), Atmel Corporation (2012d) and Texas Instruments (2012). Costings from Farnell (2012)

2.2.2 Atmel Software Framework

Atmel offer a software framework which contains basic code and device drivers for many of their XMega and AT32 devices (Atmel Corporation (2012c)). There are also many AVR application notes which provide explanations and example code for protocols like TWI, SPI and timers. These application notes are aimed at older devices like the ATTiny and ATMega and are generally written for IAR Embedded Workbench compiler, as opposed to the AVRGCC compiler used within Atmel Studio.

Chapter 3

Initial Hardware and Firmware Development

For initial development, the *Il Matto* board, designed by Steve Gunn, was used. The system has an ATMega644P clocked at 12MHz and has an on-board SD card socket.

The following section is broken down into the following parts:

1. Camera Code
2. SD Card
3. Circuit and PCB Development

3.1 Camera

The camera used is an OV7670 by OmniVision. It is mounted onto a break out board and connected to a AL422B FIFO Buffer. The breakout board has all passive components needed and a 24MHz clock mounted. The schematic for the device can be seen in appendix B.

Original code for the camera operation was given by Steve Gunn, which I used to gain the operation required. This code streamed continuous video to a TFT screen. The operation required was to take a single photo from the camera and store the data.

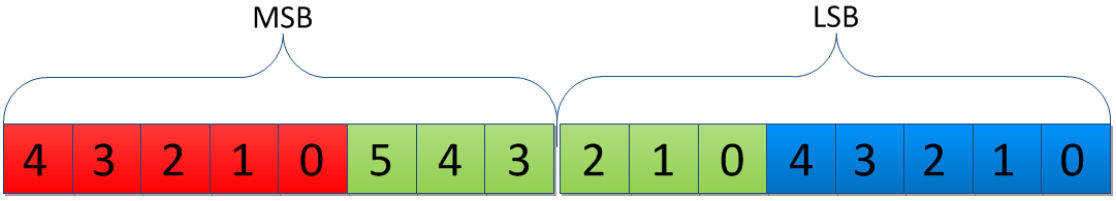

Figure 3.1: RGB565 pixel format

3.1.1 Single Camera Operation

The camera uses a SCCB Interface (OmniVision (2007)) created by OmniVision. This is almost identical to the I^2C Interface by Phillips and the two protocols are compatible. The original code used a bit-banged SCCB interface which was very slow and used up processing time. This was changed to make used of the built-in interrupt-driven I^2C interface (named TWI in Atmel AVRs)[1]. This communication bus is used to set up the control registers of the OV7670 to enable operation in the correct format. RGB565 is used in my application.

RGB565 is a 16 bit pixel representation where bits 0:4 represent the blue intensity, 5:10 is the green intensity and 11:15 represent the red intensity (see figure 3.1). This is a compact way of storing data but only allows 65536 colours. Greys can also appear to be slightly green due to the inconsistent colour ratio of the green field.

The camera must use a high speed clock in order to ensure the pixels obtained are from the same time. This makes it difficult for an AVR to be able to respond to the camera quick enough (ATMegas typically clocked at 8-12MHz). This highlights the necessity for a FIFO Buffer.

The OV7670 is set up so that the VSYNC pin goes low at the beginning of every full frame of data, and HREF is high when the data being output is valid. The pixel data is then clocked out on every rising edge of PCLK. To control the buffer, WEN (write enable) is NAND with the HREF signal. When both are high, the write enable to the buffer will be active and the data will be clocked in by PCLK. In order to acquire a full frame, the first VSYNC pin is set up to interrupt the AVR to enable WEN. The camera will output an entire frame of pixel data and store it into the buffer. When the second VSYNC is received, the WEN signal is disabled, stopping any more data being stored. The FIFO buffer now contains an entire image.

[1] I^2C , SCCB and TWI are all the same but are called differently due to Phillips owning the right to the name "I^2C"

Figure 3.2: Signals generated to control the OV7670 capture and read

To obtain the data from the buffer, the AVR sets output enable and pulses the read clock. Valid data is available on the input port while RCLK is high. All the data is then read in half a pixel at a time. The entire operation can be seen in figure 3.2.

Difficulties arose at this point with the storage of the data. The ATMega644P has 4kB of internal SRAM, but 153.6kB of memory is needed to store a single image at QVGA (320 by 240 pixels, 2 bytes per pixel) quality.

Firstly, data was sent straight to a desktop computer via a COM Port using USART. A simple desktop program was written in C# to receive and store all the data, and to make a Bitmap image from the data. This method was slow, taking around 30 seconds to transmit one uncompressed image.

The second option was to use extra memory connected to the microcontroller. An SD card is used as FAT file system so that data can be looked at by a user on a computer. Text log files are also written to aid debugging. This is discussed in section 3.2.

3.1.2 Dual Camera Operation

In order for stereovision to be successful, two cameras separated by a horizontal distance (B) will need to be driven at the same time to obtain photos within a small time frame of one another.

A major problem occurred with using the I^2C interface to set up both cameras. The camera has a set I^2C address of 21_{16}, which cannot be changed. Multiple

I^2C devices with exactly the same address cannot be used on the same bus. Two solutions to this are possible: driving one from I^2C and one from SCCB, or using an I^2C multiplexer. By using two different buses, there can be no bus contention. However, SCCB is slow and processor-hungry as it deals with the protocol bit by bit in software. This takes up memory and is not reusable for other operations.

An I^2C multiplexer sits on the bus and has multiple output buses. The master can then address the multiplexer and select whether to pass the bus to bus 0, bus 1 or not allow the data to be transferred. This saves processor time, but means a write operation has to be done to select the camera bus before being able to write to the camera. This slows down the operation, but not as much as using SCCB. The main disadvantage to the I^2C MUX is the extra hardware needed; firstly the MUX itself, but also 7 extra resistors to pull up the two extra buses and the three interrupt lines must be added.

Overall, the disadvantages posed by using a MUX are small, so a multiplexer will be used as opposed to the SCCB interface. A suitable multiplexer is the Phillips PCA9542A (Phillips (2009)).

The buffers have an output enable pin so the data bus can be shared by both cameras to the AVR. The ATMega644P offers three interrupt pins, two of which are used by the two VSYNC pins for the cameras.

Two ISRs are used to control the VSYNC signals, and when taking a photo, both frames are taken at a time period close together to capture the same scenario. The data for both images are read back individually by the AVR.

Operation to read an image is identical to using one camera. However, an ID number is passed through the functions to make a decision on the pins to use to read the buffer and to enable the output. Care was taken to avoid bus contention, but no checking procedure is explicitly in place. Both images are then read back from the buffers and stored to memory.

3.2 SD Card

To use the SD card, the FATFS library (Electronic Lives Manufacturing (2012)) was used. The library supplies all the functions for writing a FAT File System in the files *ff.c*, *ff.h*, *ffconf.h*, *diskio.c*, *diskio.h* and *integer.h*. The *diskio.h* functions control what device is being used - SD/MMC Card, USB drive etc. The *ff.h* header

	Bitmap	JPEG	PNG	GIF
Extension	*.bmp	*.jpg /*.jpeg	*.png	*.gif
Compression	No	Lossless and Lossy	Lossless ZIP	Lossy
File Size of 320 by 240 pixel Image (kB)	225	20	23	24
Bits per Pixel	8, 16, 24 or 32	24	24, 32 or 48	24, but only 256 Colours

Table 3.1: A table comparing different image formats available (Fulton (2010))

contains all the functions to write to in a FAT File system.
An SD card was chosen due to it's small size, low cost and a large data storage. The cards work using an SPI bus which can be used for other devices within the system so the card only uses one extra enable pin in hardware to function.

3.2.1 Storing Images

Many image formats are common, such as Joint Photographic Expert Group (JPEG), Portable Network Graphics (PNG), Bitmap (BMP) and Graphics Interchange Format (GIF). Table 3.1 shows a summary of some common image formats.

It is clear that the best choice for images would be either PNG or JPEG. However, these require much computational time to compress the image into the correct format. To avoid compression, and thereby save processing time, bitmap was chosen at the expense of using more memory. The data in a bitmap image is also stored in RGB format so can be read back easily when processing the data. Appendix C shows the make up of a Bitmap File that was used.

By writing the image in this format, they are then able to be opened on any operating system. This aids debugging and allows the protoyping of image algorithms in a more powerful environment. Figure 3.3 shows a photo taken by the OV7670 and stored on a SD card.

Figure 3.3: An Example Image taken using the OV7670 and stored as a Bitmap on the SD Card

3.2.2 User Interface

The ATMega 664P pinout for the dual camera operation can be seen in table 3.2. Due to a lack of available GPIO pins, an ATMega168 was added on the I^2C bus to act as a port extender. The ATMega168 accepts a read or write command. A write places the written data on Port D and a read returns any button pressed that occurred on Port C. When a button is pressed, this is stored in the ATMega168 until a read has been done. This is so the master (644P) does not miss any button presses while busy doing lengthy operations such as writing an image. The code is based on Application Note AVVR311 (Atmel Corporation (2007)), written for IAR Compiler. This code was altered to compile with GCC under Atmel Studio. AVRs contain a hardware based I^2C protocol that is interrupt based in software. The interrupt service routine of the TWI vector is a state machine which loads the data to send, stores received data, responds to acknowledges and address calls and deals with bus errors that can occur.

	Port A	Port B	Port C	Port D
0	Data 0	SD Write Protect	I^2C - SCL	No Connection
1	Data 1	SD Card Detect	I^2C - SDA	No Connection
2	Data 2	USB Data Plus	Read Clock 1	VSync 0
3	Data 3	USB Data Minus	Read Reset 1	VSync 1
4	Data 4	SPI Chip Select	Write Enable 1	Read Clock 0
5	Data 5	SPI MOSI	Write Reset 1	Read Reset 0
6	Data 6	SPI MISO	Output Enable 0	Write Enable 0
7	Data 7	SPI Clock	Output Enable 1	Write Reset 0

Table 3.2: Pin Connections of the ATMega644P for Dual Camera Operation.

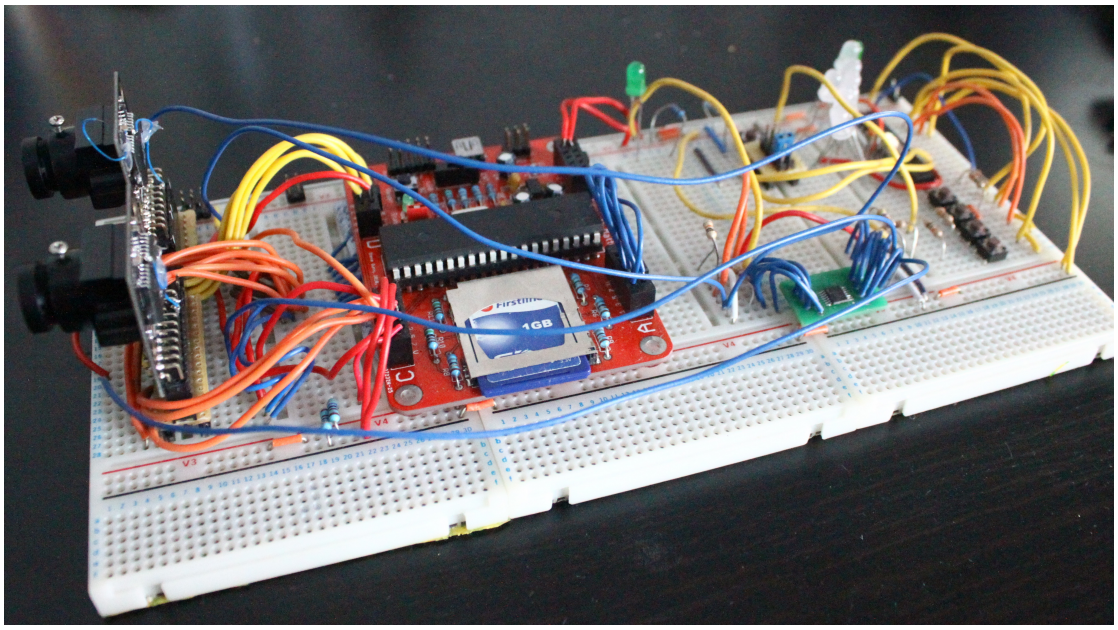

Figure 3.4: Prototype of Dual Camera operation.

3.3 Circuit and PCB Development

3.3.1 Il Matto Development

Figure B.2 shows the circuit diagram for the prototype. This uses the Il Matto development board for the main microcontroller. The prototype can be seen in figure 3.4.

Chapter 4

Investigation into Vision Algorithms

4.1 Comparison

In computer vision, there are many different ways of comparing two similar images. These include the sum of absolute differences (S.A.D.) (Hamzah et al. (2010)), the sum of squared differences (S.S.D.)(Mrovlje and Vrančić (2008)) and normalised cross correlation (N.C.C.)(Zhao et al. (2006)). Each of these methods will be explained and tested to compare them. All testing will use images seen in figure 4.1. Each test uses the same size window (50×50) to compare the two images.

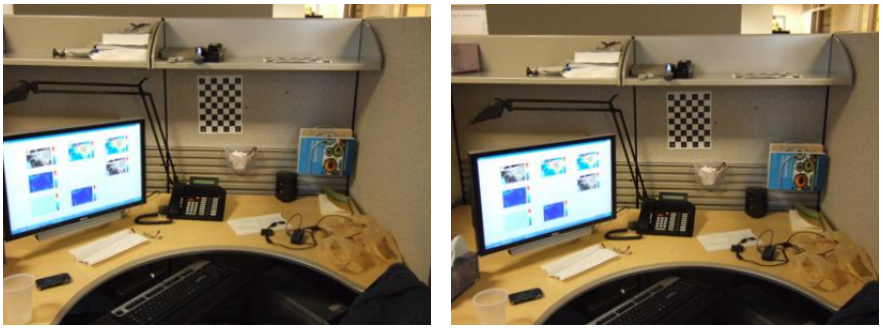

(a) Left Image (b) Right Image

Figure 4.1: Stereoscopic Test Images from MATLAB Examples

4.1.1 Sum of Absolue Differences

Given two identically sized two dimensional matrices, A, B, of dimensions I, J, SAD is defined as

$$SAD = \sum_{i=0}^{I-1} \sum_{j=0}^{J-1} A[i,j] - B[i,j] \tag{4.1}$$

This method subtracts the observed window from the expected. All differences are then added together. This algorithm is simple and requires a small amount of computation. The algorithm returns values where a small result means the two images are well matched.

4.1.2 Sum of Squared Differences

$$SSD = \sum_{i=0}^{I-1} \sum_{j=0}^{J-1} (A[i,j] - B[i,j])^2 \tag{4.2}$$

This is very similar to S.A.D. but adds more complexity by squaring each difference. This removes the ability of equally different but opposite differences cancelling each other out (grey to white of one pixel will cancel out a white to grey difference in the other with SAD). Again, a low result is a match in this case.

4.1.3 NCC

$$NCC = \frac{1}{n} \sum_{i,j} \frac{(A[i,j] - \bar{A}).(B[i,j] - \bar{B})}{\sigma_A . \sigma_B} \tag{4.3}$$

Where n is the number of pixels in A and B,
σ is the standard deviation of the image, and
$\bar{A}$ is the a average pixel value.

NCC is very similar to cross correlation, but normalised to reduce the error if one image is brighter than the other. This is common in computer vision (Tsai and Lin (2003)) and cross correlation is a often used in digital signal processing, so fast algorithms have been made to calculate this.

Unlike S.S.D. and S.A.D., the normalised cross correlation gives a high value for a match. The downside to this algorithm comes with the complexity of the equation

as it contains division and the a square root of a number in order to calculate the standard deviation. These operations are rarely implemented in hardware and are time consuming to carry out in software. They also require floating point registers and operates slowly on a microcontroller without any.

4.1.4 Comparison

To compare these equations, a 50 by 50 window taken from the right picture was compared with the left image over the entire valid range. The coordinates on the graph give the centre pixel of the calculation.

Each graph shows the correct area being identified as a match, but this also highlights the downfalls of the SAD and SSD. The figures in figure 4.2 are rotated to match the orientation of the images in figure 4.1. Each of the images is tested by attempting to match the desk phone from the right image to the entirety of the left image. The actual match should be around $(170, 176)$. An exact result cannot be estimated as the images are not matched perfectly - there isn't an exact integer of pixel difference between the images. This is the sub pixel problem (Haller and Nedevschi (2012)).

SAD results in figure 4.2(b) show large areas of matching. A minimum occurs around the location expected$(170, 175)$ of a value of 5.66×10^4. However, along the bottom of the image, where a dark area occurs below the desk in the lower part of figures 4.1, the SAD algorithm detects a greater comparison, with the lowest value in this area being 3370 at $(227, 275)$. This creates a false detection here.

SSD shows matches in the same two areas: where a match should occur and the dark area beneath the desk. The minimum value where the match should occur is 4.355×10^5 at location $(170, 176)$. However, there is a large match correlation between the dark area under the desk where the actual lowest value of 2.768×10^4 occurs at $(225, 274)$. This, again, is a false match and is a downfall of this algorithm.

The NCC results are visible in figure 4.2(c). A match can be seen at coordinate $(195, 201)$ with a peak value of 0.9654. The coordinate is different to the previous results because the cross correlation works over the boundary of the image creating more results. The dimensions of the image are 300×400, but the NCC returns an data set of dimensions 350×450 when using a window size of 50×50. To get the actual match, half of the box size must be subtracted from the returned

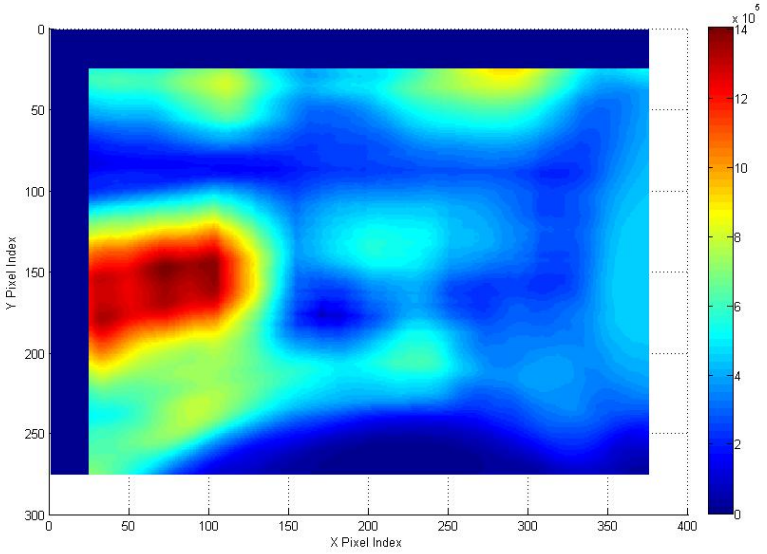

(a) S.A.D Results (Low match)

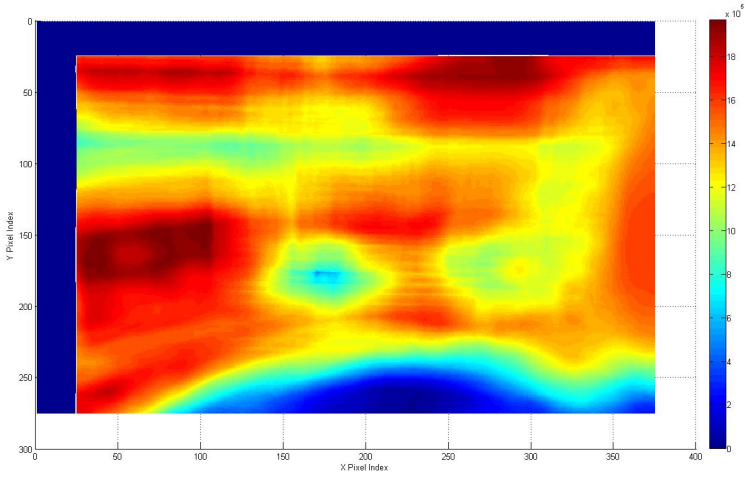

(b) S.S.D. Results (Low match)

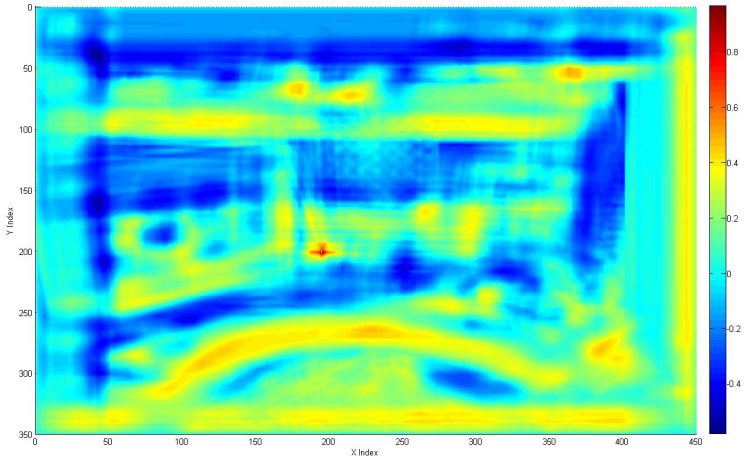

(c) N.C.C. Results (High match)

Figure 4.2: Result Graphs of Comparison Algorithms

coordinate. This means the match occurs at $(170, 176)$. With this algorithm, there is no area of the image which is close to a false detection.

4.1.5 Conclusion

It can be seen that there is a direct correlation between the complexity of the matching algorithm to the reliability of the match returned. In brightly lit, colourful environments absent of dark colours, SAD and SSD should provide a reliable result, but this cannot be guaranteed to always be the case. Therefore further development of the matching algorithm will start with using the normalised cross correlation. A comprise between complexity and reliability needs to be reached, where reliability is the more desirable of the two. Cross correlation is also a large area of research, so optimised algorithms do exist.

4.2 Range Finding

4.2.1 Derivations

By using two images separated by a horizontal distance, B, the range of an object can be found given some characteristics of the camera. The following are derivations of the equations used to calculate distance.

The problem is broken down into three parts:

1. Object is between the cameras (Figure 4.3)
2. Object is in left or right hand sides of both images (Figure 4.4)
3. Object is directly in front of a camera (Figure 4.5)

4.2.1.1 Object is between the Cameras

Derivation from Mrovlje and Vrančić (2008).

$$B = B_1 + B_2 = D\tan(\varphi_1) + D\tan(\varphi_2) \tag{4.4}$$

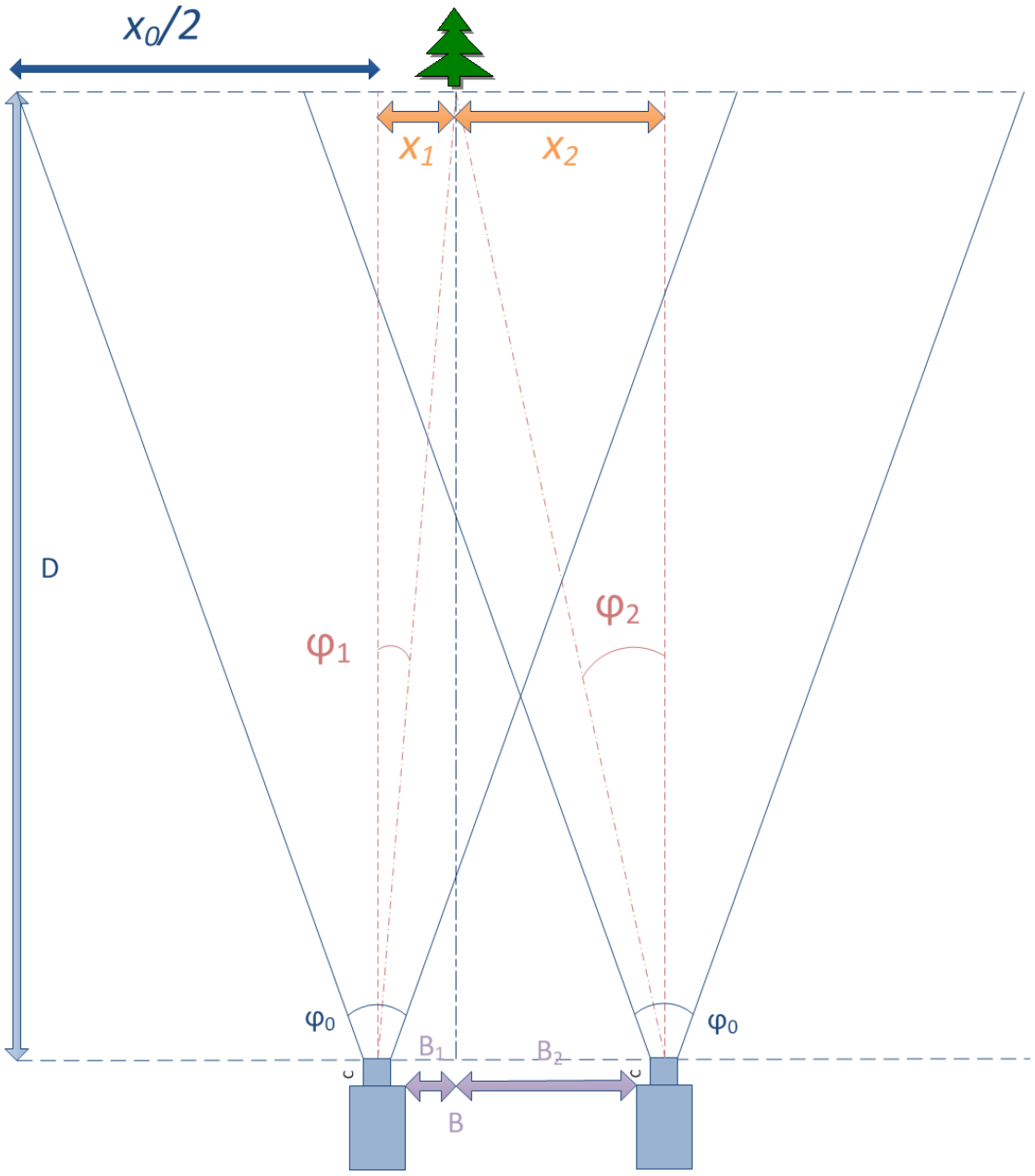

Figure 4.3: Problem 1 - Object is between the Cameras

$$D = \frac{B}{\tan(\varphi_1) + \tan(\varphi_2)} \tag{4.5}$$

$$D \tan\left(\frac{\varphi_0}{2}\right) = \frac{x_0}{2} \tag{4.6}$$

$$D \tan(\varphi_1) = x_1 \tag{4.7}$$

Dividing (4.7) by (4.6)

$$\frac{\tan(\varphi_1)}{\tan(\frac{\varphi_0}{2})} = \frac{2x_1}{x_0} \tag{4.8}$$

$$\tan(\varphi_1) = \frac{2x_1 \tan(\frac{\varphi_0}{2})}{x_0} \tag{4.9}$$

This can also be shown for the right camera:

$$\tan(\varphi_2) = \frac{-2x_2 \tan(\frac{\varphi_0}{2})}{x_0} \tag{4.10}$$

Substitution equations (4.9) and (4.10) into (4.5) gives

$$D = \frac{Bx_0}{2\tan(\frac{\varphi_0}{2})(x_1 - x_2)} \tag{4.11}$$

4.2.1.2 Object is to the same side in each camera

Derivation is based on the derivation from Tjandranegara (2005). Using figure 4.4:

$$D.\tan(\varphi_1) = x_1 \tag{4.12}$$

$$D.\tan\left(\frac{\varphi_0}{2}\right) = \frac{x_0}{2} \tag{4.13}$$

$$\frac{\tan(\varphi_1)}{\tan(\frac{\varphi_0}{2})} = \frac{2x_1}{x_0} \tag{4.14}$$

$$\varphi_1 = \arctan\left(\frac{2x_1}{x_0}\tan\left(\frac{\varphi_0}{2}\right)\right) \tag{4.15}$$

and similarly

$$\varphi_2 = \arctan\left(\frac{2x_2}{x_0}\tan\left(\frac{\varphi_0}{2}\right)\right) \tag{4.16}$$

$$\theta = \varphi_2 - \varphi_1 \tag{4.17}$$

Using the sine equality rule:

$$\frac{R}{\sin(\frac{\pi}{2} - \varphi_2)} = \frac{B}{\sin(\theta)} \tag{4.18}$$

$$R = B.\frac{\sin(\frac{\pi}{2} - \varphi_2)}{\sin(\theta)} = B\frac{\cos(\varphi_2)}{\sin(\theta)} \tag{4.19}$$

$$D = \cos(\varphi_1).R \tag{4.20}$$

Substituting (4.17) into (4.19), and then into (4.20):

$$D = B.\frac{\cos(\varphi_2).\cos(\varphi_1)}{sin(\varphi_2 - \varphi_1)} \tag{4.21}$$

Where φ_1 is defined in equation (4.15) and φ_2 is defined in equation (4.16).

4.2.1.3 Object is in front of a camera

The distance, D, in this problem is given by:

$$D = B\tan\left(\frac{\pi}{2} - \varphi_2\right) \tag{4.22}$$

Where φ_2 can be found from equation 4.16.

4.2.1.4 Summary

There are three situations that can occur. These are listed below with their equations.

Object is between the two cameras:

$$D = \frac{Bx_0}{2\tan(\frac{\varphi_0}{2})(x_1 - x_2)} \tag{4.23}$$

Object is to the same side in both images:

$$D = B.\frac{\cos(\varphi_2).\cos(\varphi_1)}{sin(\varphi_2 - \varphi_1)} \tag{4.24}$$

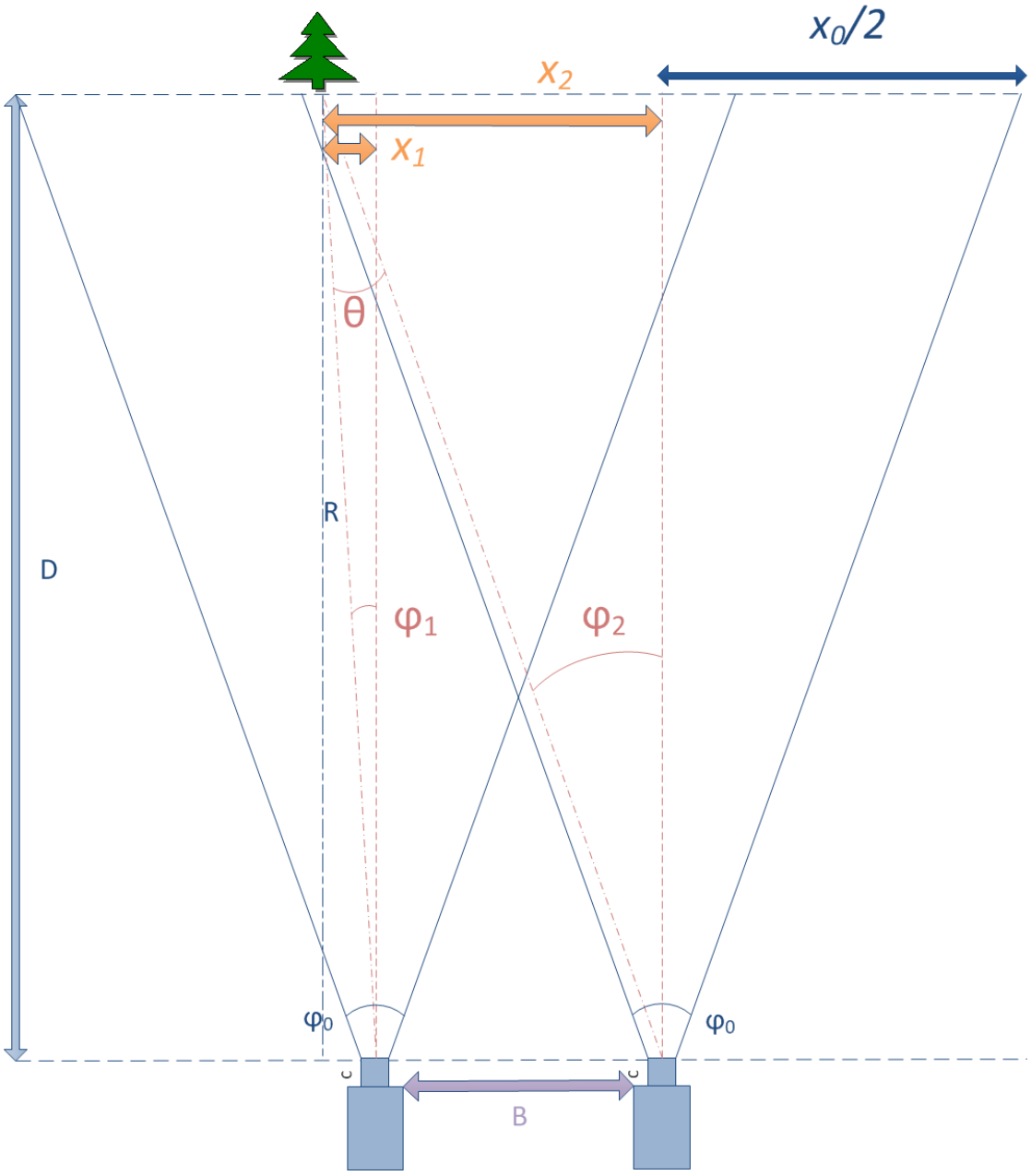

Figure 4.4: Problem 2 - Object is to the same side in both cameras

Object is directly in front of a camera:

$$D = B \tan\left(\frac{\pi}{2} - \varphi_2\right) \tag{4.25}$$

Where φ_1 is defined in equation (4.15) and φ_2 is defined in equation (4.16).

When the images have been matched, these equations can be used to calculate the range to an object.

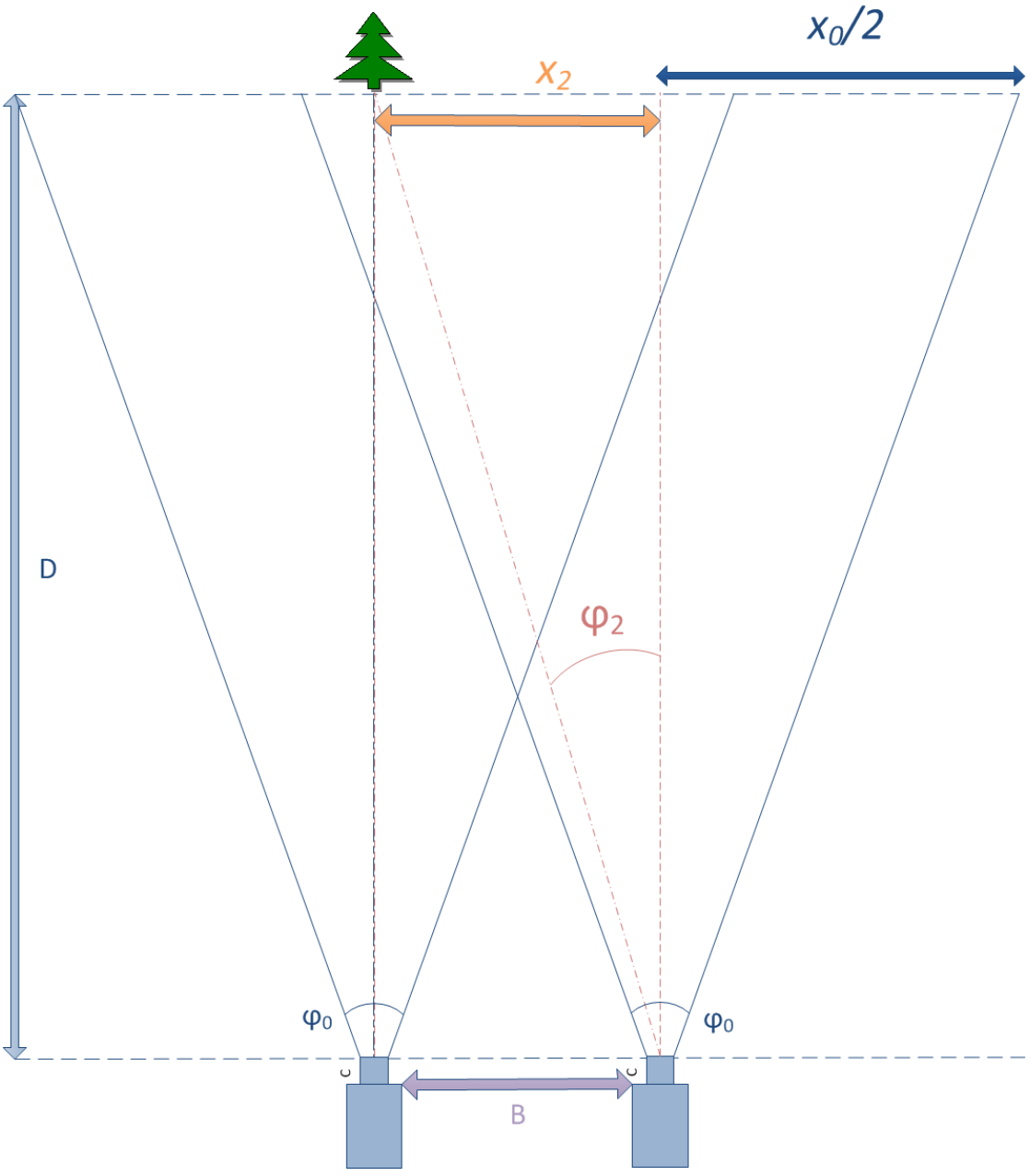

Figure 4.5: Problem 3 - Object is directly in front of a camera

Chapter 5

Conclusions and Further Work

So far, the project has addressed three aspects of the whole design: image acquisition, object matching and range finding. All these aspects have been developed separately on different platforms; on an ATMega644P or in MATLAB.

A full image can be read from a camera and stored on an SD card in a FAT32 filesystem. This gives the ability of removable memory that can be viewed on a computer to see any internal logs. Images are stored in QVGA format (320 by 240 pixels) as a bitmap image.

Multiple comparison algorithms have been investigated and compared using the same test images. It was clear that, although at a necessity of more computations, the normalised cross correlation is the best with regard to overall reliability.

Range finding equations were then derived, which use the characteristics of the camera and the separation distance between them.

The next steps will be bringing the comparison and range equations together so as to be able to choose an object in a scene and find the range to the object. Object detection algorithms need to be looked into so that an object in view can be detected and correctly located.

Robot movement also needs development. An accurate method to move a distance will be implemented with a proportional or PID controller.

A printed circuit board will also be designed. It will use the AT32UC3C0512 and contain motor drivers, I^2C multiplexer, camera connections and a TFT screen. This will then mean all modules (image acquisition, comparison, range finding

etc.) can be ported to the AVR32 and the robot can be made mobile. Further sections can then be developed such as the occupancy map and search algorithms.

All modules will be tested before being implemented. The final hardware design and development is to be completed by and the project report hand-in date is 1st May 2013.